J. Fluid Mech. (1969), *vol.* 38, *part* 1, *pp.* 39–59
Printed in Great Britain

Stability of three-dimensional laminar and turbulent shear layers

By M. LESSEN, G. HARPAVAT AND H. M. ZIEN
Department of Mechanical and Aerospace Sciences, University of Rochester, Rochester, New York, 14627

(Received 28 June 1968 and in revised form 12 December 1968)

The linear, normal mode instability of three-dimensional laminar and turbulent shear layers is studied. The flows consist of two streams semi-infinitely extended in the y-direction, flowing obliquely in the x–z plane. It is found that the stability of the flows depends on the main flow velocity components in the direction of the disturbance wave-number vector. Numerical calculations are performed to obtain the neutral stability curves. Under the usual parallel unperturbed flow assumption, the neutral stability curves pass through the origin of the α–R diagram, where α is the wave-number and R is the flow Reynolds number. It is also found that eddy viscosity has a destabilizing effect for small Reynolds numbers but a stabilizing effect at larger Reynolds numbers. Because any linear perturbation trajectory eventually leaves the unstable region of the α–R plane, it is probable that a Lin–Benney or Taylor–Goertler secondary instability ensues. Suitable components of the existing turbulence grow and develop into a large eddy system which causes rapid entrainment, giving rise to a turbulent burst. A first-order non-parallel correction is made to the neutral stability curves. The new curves have both upper and lower branches, and there exist minimum critical Reynolds numbers.

1. Introduction

Malkus (1956) postulated in his theory of turbulent shear flow that a turbulent flow is marginally stable in the Orr–Sommerfeld sense. Reynolds & Tiederman (1967) showed that the conjectures that the turbulent velocity profile has unstable or marginally stable eigenvalues were incorrect. They found that the critical Reynolds number for experimental velocity profiles (for a channel flow) is a factor of 10 greater than the flow Reynolds number. However, the assumption of neglecting the interaction term in the stability calculations (interaction between the infinitesimal wave and the background turbulence) is open to question.

The object of the present investigation is to examine the stability of laminar and free turbulent shear layers from the viewpoint of the classical theory of hydrodynamic stability. It is well established that turbulent boundary layers have characteristic mean velocity profiles and that the Reynolds stresses which shape these profiles can be attributed to a scalar eddy viscosity. We shall examine the relations between mean velocity profile, the eddy viscosity and some

three-dimensional oscillations, for a special case of a three-dimensional shear layer.

A turbulent layer has a sharp and contorted edge, known as the super layer. Our main idea is that the whole turbulent shear layer behaves as a special laminar layer, and that the contortions are similar to Tollmien–Schlichting waves. In an oscillating turbulent flow, the massaging of small eddies by the oscillation creates Reynolds stresses. The concept of eddy viscosity offers an easy method of expressing these stresses. Townsend (1956) and other researchers have shown that for free flows the eddy viscosity may be assumed approximately constant at the centre of the flow. However, the eddy viscosity cannot remain constant throughout the flow, due to the variable nature of turbulent fluctuations. Two things can happen. Either the Reynolds stresses, i.e. eddy viscosity, instantaneously follows the rate of strain, or it responds with some lag. A lag would lead to the concept of an eddy viscosity varying with the frequency and wave-number of the wave. Provided the length scale of the oscillations is large compared with the length scale of the turbulent eddies, it is reasonable to assume the same form for eddy viscosity as that used to express the interaction of the mean flow and the turbulence. This assumption will be made in deriving the disturbance equations. For simplicity, we shall assume that the eddy viscosity is a scalar quantity, and that it varies with the distance across the flow. We shall assume a suitable eddy viscosity variation consistent with mixing length theory, and the experimental data available for free boundary layers. Since our mathematical methods are limited, we shall postulate some suitable eddy viscosity distribution and examine the consequences. We shall vary the ratio of ordinary to eddy viscosity at the centre of the flow and evaluate its relative influence on the amplification of waves. A similar problem for a laminar shear layer has been studied by Yamada (1960, 1965). For comparison, the stability of a laminar shear layer will be included along with the turbulent case.

2. Mean equations of motion

Consider two streams of a viscous incompressible fluid, semi-infinitely extended in the y-direction (figure 1). Initially, the upper stream, $y > 0$, has a mean velocity $\overline{U}_1^*$ whose x and z components are $\overline{U}_1 = |\overline{U}_1^*| \cos\theta_1$ and $\overline{W}_1 = |\overline{U}_1^*| \sin\theta_1$ respectively. The lower stream has a uniform velocity $\overline{U}_2^*$ whose x and z components are $\overline{U}_2 = |\overline{U}_2^*| \cos\theta_2$ and $\overline{W}_2 = |\overline{U}_2^*| \sin\theta_2$ respectively. The streams contact each other initially along the z-axis. Thus, the mean velocity field inside the turbulent boundary layer is twisted and is independent of z. Assuming that the stresses are proportional to the rate of strain, for a viscous, incompressible fluid with a variable eddy viscosity, we have the following set of mean equations of motion:

Continuity:
$$\frac{\partial \overline{U}}{\partial x} + \frac{\partial \overline{V}}{\partial y} = 0. \tag{1}$$

Motion:
$$\overline{U}\frac{\partial \overline{U}}{\partial x} + \overline{V}\frac{\partial \overline{U}}{\partial y} = -\frac{1}{\rho}\frac{\partial \overline{P}}{\partial x} + (\nu + \nu_t)\left(\frac{\partial^2 \overline{U}}{\partial x^2} + \frac{\partial^2 \overline{U}}{\partial y^2}\right) + \frac{\partial \nu_t}{\partial y}\left(\frac{\partial \overline{U}}{\partial y} + \frac{\partial \overline{V}}{\partial x}\right), \tag{2}$$

$$\overline{U}\frac{\partial \overline{V}}{\partial x}+\overline{V}\frac{\partial \overline{V}}{\partial y}=-\frac{1}{\rho}\frac{\partial \overline{P}}{\partial y}+(\nu+\nu_t)\left(\frac{\partial^2 \overline{V}}{\partial x^2}+\frac{\partial^2 \overline{V}}{\partial y^2}\right)+2\frac{\partial \nu_t}{\partial y}\frac{\partial \overline{V}}{\partial y}, \tag{3}$$

$$\overline{U}\frac{\partial \overline{W}}{\partial x}+\overline{V}\frac{\partial \overline{W}}{\partial y}=(\nu+\nu_t)\left(\frac{\partial^2 \overline{W}}{\partial x^2}+\frac{\partial^2 \overline{W}}{\partial y^2}\right)+\frac{\partial \nu_t}{\partial y}\frac{\partial \overline{W}}{\partial y}, \tag{4}$$

where ν is the kinematic viscosity, ρ = density, $\nu_t(y)$ = eddy viscosity distribution and $\overline{U}(x,y)$, $\overline{V}(x,y)$ and $\overline{W}(x,y)$ are the mean velocity components in the x, y and z directions respectively. The case $\nu_t = 0$ corresponds to that of laminar flow.

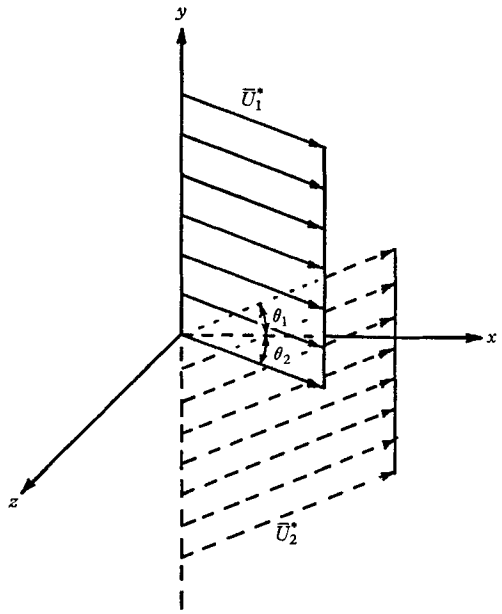

FIGURE 1. Initial velocity profile (uniform in the z-direction).

Using an order of magnitude analysis and neglecting small order quantities, we finally get the following set of equations for the mean motion:

$$\frac{\partial \overline{U}}{\partial x}+\frac{\partial \overline{V}}{\partial y}=0, \tag{5}$$

$$\overline{U}\frac{\partial \overline{U}}{\partial x}+\overline{V}\frac{\partial \overline{U}}{\partial y}=(\nu+\nu_t)\frac{\partial^2 \overline{U}}{\partial y^2}+\frac{\partial \nu_t}{\partial y}\frac{\partial \overline{U}}{\partial y}, \tag{6}$$

$$U\frac{\partial \overline{W}}{\partial x}+\overline{V}\frac{\partial \overline{W}}{\partial y}=(\nu+\nu_t)\frac{\partial^2 \overline{W}}{\partial y^2}+\frac{\partial \nu_t}{\partial y}\frac{\partial \overline{W}}{\partial y}. \tag{7}$$

The above set of mean equations of motion could also be derived from Reynolds equations for a turbulent flow by expressing Reynolds stresses in terms of eddy viscosity and mean velocity gradients.

(i) $\nu_t = 0$ (*laminar flow*). From the continuity equation, one can define a stream function with

$$\overline{U}=\frac{\partial \psi}{\partial y} \quad \text{and} \quad \overline{V}=-\frac{\partial \psi}{\partial x}. \tag{8}$$

Let $$\psi = \sqrt{(\nu x \overline{U}_1)} f(\eta) \tag{9}$$

and $$\overline{W} = \overline{U}_1 (dg(\eta)/d\eta), \tag{10}$$

where $$\eta = y/(\nu x/\overline{U}_1)^{\frac{1}{2}} = y/l. \tag{11}$$

The velocity components, therefore, are

$$\left.\begin{aligned} \overline{U} = \overline{U}_1 f', \quad \overline{V} = \tfrac{1}{2}(\nu \overline{U}_1/x)^{\frac{1}{2}}(\eta f' - f) \\ \text{and} \qquad \overline{W} = \overline{U}_1 g', \end{aligned}\right\} \tag{12}$$

where the superscript 'prime' denotes differentiation with respect to η.

Equations (6) and (7) then become

$$ff'' + 2f''' = 0 \tag{13}$$

and $$fg'' + 2g''' = 0, \tag{14}$$

the boundary conditions, on which are

$$f' \to 1, \quad g' \to \frac{\overline{W}_1}{\overline{U}_1} = a_1, \quad \eta \to \infty; \tag{15}$$

and $$f' \to \overline{U}_2/\overline{U}_1, \quad g' \to \overline{W}_2/\overline{U}_2 = a_2, \quad \eta \to -\infty. \tag{16}$$

It should be noted that the x-component, $\overline{U}$, satisfies the Blasius equation and is determined by the initial velocity components in the x-direction. However, the z-component, $\overline{W}$, is determined by the initial velocity components in both x- and z-directions. Solution of (13 may be obtained numerically by the method given by Lessen (1950).

The velocity component in the z-direction is then given by

$$g'(\eta) = c_1 f'(\eta) + c_2, \tag{17}$$

where c_1 and c_2 are integration constants. In particular, when the x-component of the initial velocities of both streams are equal, then f' is constant. The velocity distribution is given by

$$f' = 1, \quad g'(\eta) = a_1 - \frac{a_1 - a_2}{2} \operatorname{erfc}\left(\frac{\eta}{2}\right). \tag{17a}$$

(ii) $\nu_t \neq 0$ (*turbulent flow*). Now the functional form of the self-preserving flow is

$$F = F(y/x) \tag{18}$$

(Townsend 1956). Therefore we select the new independent variable η as

$$\eta = \Lambda y/x, \tag{19}$$

where Λ is a scale factor and is determined by the scale of turbulence. From (5) we can define a stream function ψ with

$$\overline{U} = \frac{\partial \psi}{\partial y} \quad \text{and} \quad \overline{V} = -\frac{\partial \psi}{\partial x}. \tag{20}$$

Let $$\psi = \overline{U}_1 x \phi(\eta)/\Lambda \tag{21}$$

and $$\overline{W} = \overline{U}_1 f'(\eta). \tag{22}$$

The velocity components, therefore, are

$$\overline{U} = \overline{U}_1\phi'(\eta), \quad \overline{V} = -\overline{U}_1[\phi(\eta)-\eta\phi'(\eta)]/\Lambda \quad \text{and} \quad \overline{W} = \overline{U}_1 f'(\eta). \tag{23}$$

Equations (6) and (7) then become

$$\phi(\eta)\phi''(\eta)+\frac{\sigma}{1+\sigma}\phi'''(\eta)+\frac{1}{1+\sigma}\frac{\partial}{\partial\eta}[G(\eta)\phi''(\eta)] = 0, \tag{24}$$

$$\phi(\eta)f''(\eta)+\frac{\sigma}{1+\sigma}f'''(\eta)+\frac{1}{1+\sigma}\frac{\partial}{\partial\eta}[G(\eta)f''(\eta)] = 0, \tag{25}$$

where $\nu_t = \nu_0 G(\eta)$, $\sigma = \nu/\nu_0$ and $\Lambda^2 = \overline{U}_1 x/(\nu+\nu_0) = R_x$, which is essentially a constant when a fully developed turbulent flow is considered.

The boundary conditions are

$$\phi' \to 1, \quad f'(\eta) \to \overline{W}_1/\overline{U}_1 = a_1, \quad \text{as} \quad \eta \to \infty, \tag{26}$$

and

$$\phi' \to \overline{U}_2/\overline{U}_1, \quad f'(\eta) \to \overline{W}_2/\overline{U}_1 = a_2, \quad \text{as} \quad \eta \to -\infty. \tag{27}$$

For a particular case in which the x-components of the initial velocity of both streams are equal, $\phi'(\eta)$ is a constant; and the velocity distribution is given by

$$\phi'(\eta) = 1 \tag{28}$$

and

$$\eta f''(\eta)+\frac{\sigma+G(\eta)}{1+\sigma}f''(\eta)+\frac{1}{1+\sigma}G'(\eta)f''(\eta) = 0. \tag{29}$$

3. Disturbance equations

Assuming that the flow is parallel, and that the disturbances to the flow are small, the dimensionless velocity components may be written as

$$u = \overline{U}+u_1, \quad v = v_1, \quad w = \overline{W}+w_1 \tag{30}$$

and the dimensionless pressure as

$$p = \overline{p}+p_1, \tag{31}$$

where the subscript '1' denotes the disturbance quantities. By substituting the above quantities into the three-dimensional equations of motion, by assuming the same form for eddy viscosity as that used to express the interaction of the mean flow and turbulence, by subtracting the mean flow quantities from the resulting equations and by taking only terms linear in the disturbance, one obtains the following set of disturbance equations:

$$\frac{\partial u_1}{\partial x}+\frac{\partial v_1}{\partial y}+\frac{\partial w_1}{\partial z} = 0, \tag{32}$$

$$\frac{\partial u_1}{\partial t}+\overline{U}\frac{\partial u_1}{\partial x}+\overline{W}\frac{\partial u_1}{\partial z}+v_1\frac{\partial \overline{U}}{\partial y} = -\frac{\partial p_1}{\partial x}+\frac{\sigma+G(\eta)}{R\sigma}\nabla^2 u_1+\frac{G'(\eta)}{R\sigma}\left(\frac{\partial u_1}{\partial y}+\frac{\partial v_1}{\partial x}\right), \tag{33}$$

$$\frac{\partial v_1}{\partial t}+\overline{U}\frac{\partial v_1}{\partial x}+\overline{W}\frac{\partial v_1}{\partial z} = -\frac{\partial p_1}{\partial y}+\frac{\sigma+G(\eta)}{R\sigma}\nabla^2 v_1+\frac{2G'(\eta)}{R\sigma}\frac{\partial v_1}{\partial y}, \tag{34}$$

$$\frac{\partial w_1}{\partial t}+\overline{U}\frac{\partial w_1}{\partial x}+\overline{W}\frac{\partial w_1}{\partial z}+v_1\frac{\partial \overline{W}}{\partial y} = -\frac{\partial p_1}{\partial z}+\left(\frac{\sigma+G(\eta)}{R\sigma}\right)\nabla^2 w_1+\frac{G'(\eta)}{R\sigma}\left(\frac{\partial v_1}{\partial z}+\frac{\partial w_1}{\partial y}\right), \tag{35}$$

where $R = \bar{U}_1 l_0/\nu$ is the Reynolds number and l_0 is the characteristic length $l_0 = (\nu x/\bar{U}_1)^{\frac{1}{2}}$ for linear flow; $l_0 = x/\Lambda$ for turbulent flow.

Let the disturbances be three-dimensional plane waves of the form

$$\{u_1, v_1, w_1, p_1\} = \{s(y), g(y), h(y), \pi(y)\} \exp[i(\alpha x + \beta z - \alpha c t)], \tag{36}$$

where $c = c_r + ic_i$ is complex. Then, upon substituting (36) in (33), (34) and (35), and using the Squire transformation (Squire 1933), we finally obtain the following disturbance equation:

$$(\bar{U} - \tilde{c})(g'' - \tilde{\alpha}^2 g) - \bar{U}'' g = -\frac{i(\sigma + G(\eta))}{\tilde{\alpha} R \sigma}(g^{\mathrm{IV}} - 2\tilde{\alpha}^2 g'' + \tilde{\alpha}^4 g) - \frac{2iG'(\eta)}{\tilde{\alpha} R \sigma}(g''' - \tilde{\alpha}^2 g') - \frac{iG''(\eta)}{\tilde{\alpha} R \sigma}(g'' + \tilde{\alpha}^2 g), \tag{37}$$

where

$$\tilde{\alpha}\bar{U} = \alpha \bar{U} + \beta \bar{W},$$

$$\tilde{\alpha}\tilde{c} = \alpha c,$$

and

$$\tilde{\alpha}^2 = \alpha^2 + \beta^2.$$

For boundary conditions on (37), it suffices to specify that g is bounded throughout the flow field.

Because (37) is of the fourth order, there exists a set of four linearly independent solutions of the equation:

$$g = c_1 g_1 + c_2 g_2 + c_3 g_3 + c_4 g_4. \tag{38}$$

The nature of the solutions g_3 and g_4 at large $\tilde{\alpha}R$ can be investigated by W.K.B. method, by introducing the following transformation into (37):

$$g(y) = \exp(\int p\, dy). \tag{39}$$

Here p is to be expanded as follows:

$$p = (\tilde{\alpha}R)^{\frac{1}{2}} p_0 + p_1 + (\tilde{\alpha}R)^{-\frac{1}{2}} p_2 + \ldots. \tag{40}$$

Then, after inserting (39) into (37), and using (40), we obtain

$$g_3 \simeq \{(\bar{U} - \tilde{c})\sigma^2\}^{-\frac{5}{4}} \exp[-\int (i\tilde{\alpha}R(\bar{U} - \tilde{c}))^{\frac{1}{2}} dy], \tag{41}$$

$$g_4 \simeq \{(\bar{U} - \tilde{c})\sigma^2\}^{-\frac{5}{4}} \exp[\int (i\tilde{\alpha}R(\bar{U} - \tilde{c}))^{\frac{1}{2}} dy]. \tag{42}$$

It should be noted that when

$$y \to -\infty, \quad g_3 \to \infty, \quad \text{and} \quad y \to \infty, \quad g_4 \to \infty.$$

Because for large $\tilde{\alpha}R$, g_3 and g_4 are each unbounded somewhere in the flow field, they may be neglected in the solution of equation (37) for 'large' Reynolds numbers. In fact, in our exact numerical analysis, we also have found that, for $\tilde{\alpha}R > 10$, the contribution from these viscous solutions to the eigenvalues is almost negligible.

For the case where the wave-number vector is in the z-direction, the disturbance quantity may be expressed in the form

$$Q = g(y) \exp[i(\beta z - \beta c t)] \tag{43}$$

then $\tilde{\alpha}$ and $\tilde{c}$ in (37) correspond respectively to β and c of equation (43). Only the velocity component in the z-direction is required in the stability consideration. As is seen from (37), the stability of the flow is determined by the mean flow velocity in the direction of the wave-number vector. This case is considered in our stability investigation.

4. Boundary conditions

For $\theta = \theta_1 = \theta_2 = 45°$, $\tilde{U}(y) \to \pm 1$ as $y \to \pm\infty$ and $\tilde{U}''$, $G(y)$, $G'(y)$, $G''(y)$ all tend to zero as $y \to \pm\infty$. Therefore, at large y, the proper boundary conditions are

$$g_{+\infty} = c_1 \exp(-\tilde{\alpha}y) + c_2 \exp(-\tilde{\beta}_1 y), \tag{44}$$

$$g_{-\infty} = c_3 \exp(\tilde{\alpha}y) + c_4 \exp(\tilde{\beta}_2 y), \tag{45}$$

where $\tilde{\beta}_1^2 = \tilde{\alpha}^2 + i(1-\tilde{c})\tilde{\alpha}R$ and $\tilde{\beta}_2^2 = \tilde{\alpha}^2 - i(1+\tilde{c})\tilde{\alpha}R$.

Equations (44) and (45) give the following four boundary conditions:

$$g''_{+\infty} + (\tilde{\alpha}+\tilde{\beta}_1) g'_{+\infty} + \tilde{\alpha}\tilde{\beta}_1 g_{+\infty} = 0, \tag{46}$$

$$g'''_{+\infty} + (\tilde{\alpha}+\tilde{\beta}_1) g''_{+\infty} + \tilde{\alpha}\tilde{\beta}_1 g'_{+\infty} = 0, \tag{47}$$

$$g''_{-\infty} - (\tilde{\alpha}+\tilde{\beta}_2) g'_{-\infty} + \tilde{\alpha}\tilde{\beta}_2 g_{-\infty} = 0, \tag{48}$$

$$g'''_{-\infty} - (\tilde{\alpha}+\tilde{\beta}_2) g''_{-\infty} + \tilde{\alpha}\tilde{\beta}_2 g_{-\infty} = 0. \tag{49}$$

In the flow under investigation, both $\tilde{U}$ and $\tilde{U}''$ are real and antisymmetric and $\tilde{c}_r = 0$ (appendix); both $\tilde{U} - \tilde{c}_r$ and $\tilde{U}''$ are odd functions of y for the real part and even functions for the imaginary part. Therefore, by the proper choice of the multiplying coefficients, each of the four independent solutions of the stability equation will be such that either the real part is even and the imaginary part odd, or *vice versa*.

Since the equations and boundary conditions are homogeneous, and since both sets of symmetry conditions can be obtained from each other by multiplying through with an imaginary constant, either symmetry will yield the same stability characteristics. Without loss of generality, it can then be assumed that all the four independent solutions are such that their real parts are symmetric and the imaginary parts antisymmetric. Thus the relevant boundary condition determinant is

$$\begin{vmatrix} A_1 & A_2 & A_3 & A_4 \\ B_1 & B_2 & B_3 & B_4 \\ D_1 & D_2 & D_3 & D_4 \\ E_1 & E_2 & E_3 & E_4 \end{vmatrix} = 0, \tag{50}$$

where

$$\begin{aligned} A_n &= g''_{nr+\infty} + (\tilde{\alpha}+\beta_r) g'_{nr+\infty} - \beta_i g'_{ni+\infty} + \tilde{\alpha}(\beta_r g_{nr+\infty} - \beta_i g_{ni+\infty}), \\ B_n &= g''_{ni+\infty} + (\tilde{\alpha}+\beta_r) g'_{ni+\infty} + \beta_i g'_{nr+\infty} + \tilde{\alpha}(\beta_r g_{ni+\infty} + \beta_i g_{ni+\infty}), \\ D_n &= g'''_{nr+\infty} + (\tilde{\alpha}+\beta_r) g''_{nr+\infty} - \beta_i g''_{ni+\infty} + \tilde{\alpha}(\beta_r g'_{nr+\infty} - \beta_i g'_{ni+\infty}), \\ E_n &= g'''_{ni+\infty} + (\tilde{\alpha}+\beta_r) g''_{ni+\infty} + \beta_i g''_{nr+\infty} + \tilde{\alpha}(\beta_r g'_{ni+\infty} + \beta_i g'_{nr+\infty}), \end{aligned}$$

where n varies from 1 to 4 and $\tilde{\beta}_1 = \beta_r + i\beta_i$.

When the integration is started from boundaries at infinity, we have in this case:

$$g = c_1 g_{I1} + c_2 g_{I2} \quad \text{for} \quad y > 0, \tag{51}$$

and

$$g = c_3 g_{II1} + c_4 g_{II2} \quad \text{for} \quad y < 0, \tag{52}$$

where

$$g_{I1+\infty} = \exp(-\tilde{\alpha} y), \quad g_{I2+\infty} = \exp(-\tilde{\beta}_1 y),$$
$$g_{II1-\infty} = \exp(\tilde{\alpha} y), \quad g_{II2-\infty} = \exp(\tilde{\beta}_2 y). \tag{53}$$

Using the symmetry property of $g(y)$, it can again be shown that the flow under investigation is equally stable or unstable for either the real part of $g(y)$ symmetric and imaginary part antisymmetric or *vice versa*. Then the relevant boundary condition determinant at the centre of the flow is:

$$\begin{vmatrix} g_{I1i}(0) & g_{I1r}(0) & g_{I2i}(0) & g_{I2r}(0) \\ g'_{I1r}(0) & -g'_{I1i}(0) & g'_{I2r}(0) & -g'_{I2i}(0) \\ g''_{I1i}(0) & g''_{I1r}(0) & g''_{I2i}(0) & g''_{I2r}(0) \\ g'''_{I1r}(0) & -g'''_{I1i}(0) & g'''_{I2r}(0) & -g'''_{I2i}(0) \end{vmatrix} = 0, \tag{54}$$

where subscripts r and i represent real and imaginary parts respectively.

5. Numerical integration

5.1. *Mean velocity distribution for turbulent flow*

Since the exact data for the distribution of $G(\eta)$ are not available, we have selected $G(\eta)$ with some assumptions. These are as follows. (i) Eddy viscosity must go to zero at $\eta = \pm\infty$, since the outer fluid is laminar. (ii) Due to the symmetry of turbulent fluctuations in the two streams, the distribution of eddy viscosity should be symmetric in the η co-ordinate. From mixing length theory, the eddy viscosity can be expressed as

$$\nu_t = l^2 \left| \frac{du}{d\eta} \right|, \tag{55}$$

where l is the mixing length and is constant. Since in our case the point of inflexion of the velocity is at $\eta = 0$, the eddy viscosity is maximum at $\eta = 0$ and decreases as $|\eta|$ increases. Now, for a constant eddy viscosity, $G(\eta) = 1$, the velocity profile is an error function, and therefore

$$\frac{du}{d\eta} = c_1 \exp(-\eta^2/2).$$

This suggests that a plausible distribution of eddy viscosity may be of the form

$$\nu_t = \nu_0 \exp(-A\eta^2),$$

where 'A' is a constant and its approximate value is $\frac{1}{2}$. Many numerical experiments were performed, trying different eddy viscosity distributions like $\exp(-A\eta^4)$, $\exp(-A\eta^6)$, etc. It was observed that the distribution $\exp(-A\eta^2)$ with $A = 0{\cdot}45$ gives the best match with the experimental results available (Liepman & Laufer 1947). Therefore, $G(\eta) = \nu_0 \exp(-0{\cdot}45\eta^2)$ has been taken in all the numerical calculations. After substituting the expression for $G(\eta)$,

the solution of (29) is

$$f' = c_1 \int \exp\left[-\beta\eta^2\right]/\{\sigma^{(1+B/A)} + \nu_0^{(1+B/A)} \exp\left[-(A+B)\,\eta^2\right]\} d\eta + c_2$$

where c_1 and c_2 are integration constants and $B = (1+\sigma)/2\sigma$. The velocity distribution for three values of σ, namely $\sigma = 0{\cdot}50$, $\sigma = 0{\cdot}25$ and $\sigma = 0{\cdot}10$, have been calculated, and these are plotted in figures 2, 3 and 4. The slopes of velocity at the origin, for various σ, are tabulated in table 1.

σ	$f''(0)$
0·50	0·7547151334
0·25	0·7459429921
0·10	0·7387606073

TABLE 1. First derivative of velocity at the centre of the flow for various σ.

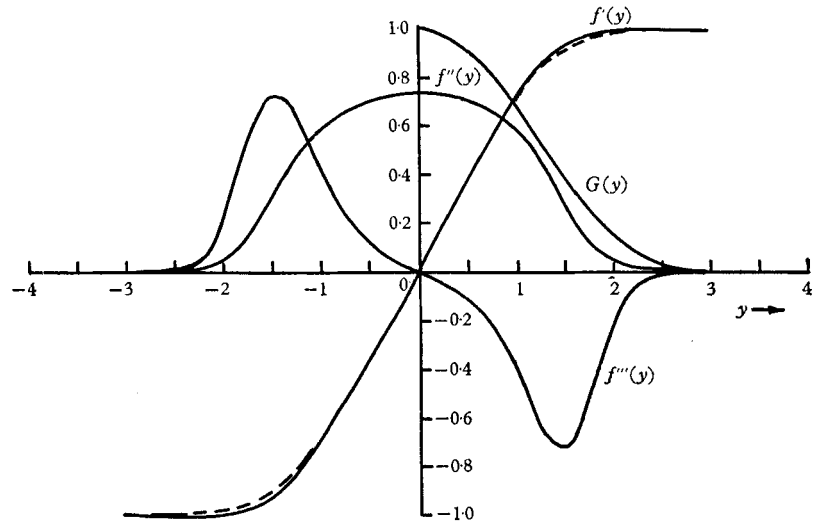

FIGURE 2. Mean velocity, its first two derivatives and the eddy viscosity distribution for $\sigma = 0{\cdot}10$: – – –, experimental velocity profile.

5.2. *Inviscid stability*

(i) *Laminar flow.* In the limit $R \to \infty$, (27) reduces to

$$(\tilde{U} - \tilde{c})(g'' - \tilde{\alpha}^2 g) - \tilde{U}'' g = 0. \tag{56}$$

For neutral oscillation $\tilde{c} = 0$ (appendix), therefore, by the transformation

$$G = g'/g, \tag{57}$$

the equation becomes

$$G' = \tilde{\alpha}^2 + \tilde{U}''/\tilde{U} - G^2. \tag{58}$$

One sees that, for the velocity distribution given by $\tilde{U} = \operatorname{erf}(\frac{1}{2}y)$ the singularity in the above equation is removable, since $\tilde{U}'' \to 0$ as $\tilde{U} \to 0$. In fact, by taking the limit $y \to 0$, $\tilde{U}''/\tilde{U} = -\frac{1}{2}$. The boundary conditions for G are

$$\left.\begin{aligned} G &= \tilde{\alpha}, \quad \text{as} \quad y \to -\infty, \\ G &= -\tilde{\alpha}, \quad \text{as} \quad y \to +\infty. \end{aligned}\right\} \tag{59}$$

Since the velocity is an odd function, g is either an even function or an odd function; therefore,

$$G = 0 \quad \text{at} \quad y = 0.$$

At large y, $\tilde{U} \to 1$ and $\tilde{U}'' = -(y/2\sqrt{\pi}) \exp[-\frac{1}{4}y^2]$; therefore, the asymptotic solution for G can be written as

$$G(y) = G_0 + G_1(y) + G_2(y) + \ldots, \tag{60}$$

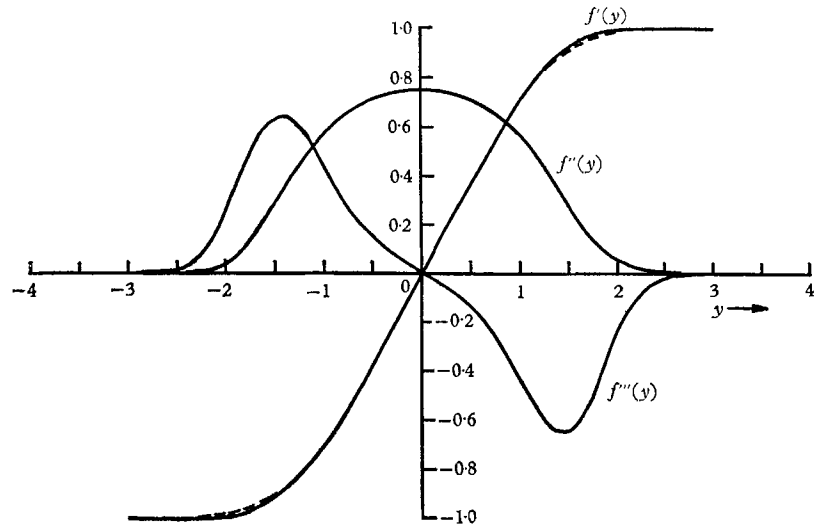

FIGURE 3. Mean velocity and its first two derivatives for $\sigma = 0{\cdot}25$: – – –, experimental velocity profile.

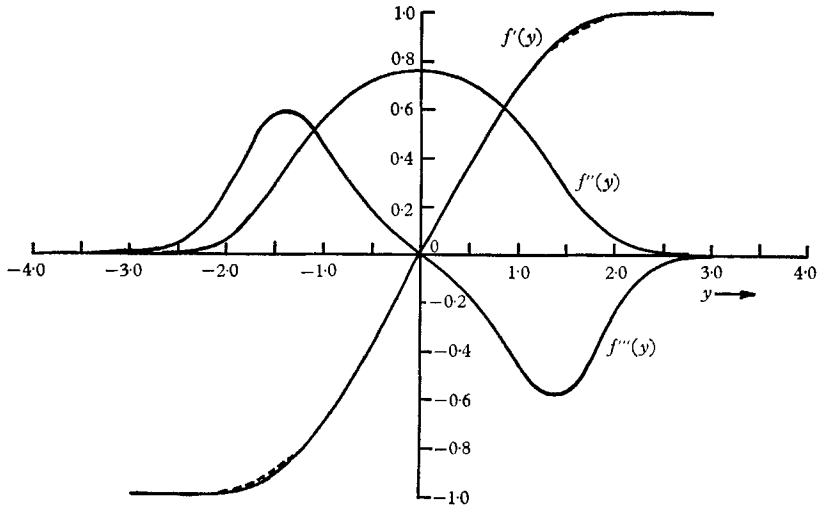

FIGURE 4. Mean velocity and its first two derivatives for $\sigma = 0{\cdot}50$: – – –, experimental velocity profile.

where G_k is of the order $(\exp[-\frac{1}{4}y^2])^k$. The first approximation is $G_0 = -\alpha$ at large y, and the second is

$$G_1 = (1/\sqrt{\pi})\exp[-\tfrac{1}{4}y^2] - 2\tilde{\alpha}^2\exp[2(\tilde{\alpha}y + 2\tilde{\alpha})]\operatorname{erf}(\tfrac{1}{2}y + 2\tilde{\alpha}). \tag{61}$$

The Adam–Bashforth method was used for finding the neutral wave-number $\tilde{\alpha}$. The integration started from the asymptotic value for G at large y. The

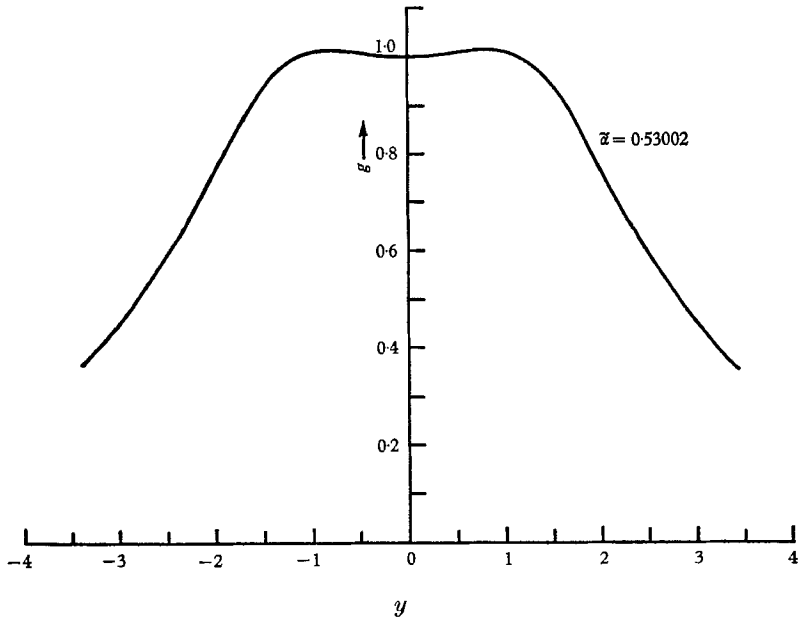

FIGURE 5. Inviscid instability disturbance function for $\sigma = 0{\cdot}10$.

σ	$\tilde{U}''(0)/\tilde{U}(0)$	$\tilde{U}'''(0)/\tilde{U}(0)$	$\tilde{U}^{iv}(0)/\tilde{U}(0)$	$\tilde{\alpha}$
0·50	−0·3933808205	−1·891382120	8·988590344	0·5837
0·25	−0·2720704232	−2·325791024	2·690533170	0·5539
0·10	−0·1731597638	−2·548675155	−3·464580769	0·5300

TABLE 2. Inviscid instability eigenvalues for various σ.

neutral wave-number was found to be $\tilde{\alpha}_5 = 0{\cdot}5175$. After scaling, Yamada's (1960) result has the same value.

(ii) *Turbulent flow.* The inviscid disturbance equation for a turbulent flow is of the same form as that for a laminar flow. For neutral stability, g is symmetric and the boundary condition at infinity is

$$g'(\infty) + \tilde{\alpha}g(\infty) = 0. \tag{62}$$

Integration can be started by taking $g(0) = 1$, and the boundary condition is satisfied at infinity. The typical disturbance function $g(y)$ for $\sigma = 0{\cdot}1$ has been plotted in figure 5 and the eigenvalues are tabulated in table 2.

5.3. *Viscous instability*

Since we have taken the real part of all the four independent solutions to be symmetric and imaginary, part anti-symmetric (for the derivation of boundary conditions determinant), without loss of generality, the four solutions at $y = 0$ may be assumed to be of the following form:

$$\left.\begin{array}{llll} g_1(0) = 1, & g_1'(0) = 0, & g_1''(0) = 0, & g_1'''(0) = 0, \\ g_2(0) = 0, & g_2'(0) = i, & g_2''(0) = 0, & g_2'''(0) = 0, \\ g_3(0) = 0, & g_3'(0) = 0, & g_3''(0) = 1, & g_3'''(0) = 0, \\ g_4(0) = 0, & g_4'(0) = 0, & g_4''(0) = 0, & g_4'''(0) = i. \end{array}\right\} \tag{63}$$

Although it might have saved computation time to take only two asymptotic solutions at large y, and to integrate backward, this procedure would have

σ	R_t	R	$\tilde{\alpha}$
0·25	8·3	41·5	0·29
0·10	8·22	90·5	0·27

TABLE 3. Minimum critical Reynolds numbers with the non-parallel correction.

$\tilde{\alpha}$	R	$\tilde{\alpha}\tilde{c}_i$
0·10	0·798253	0·0
0·25	2·47921	0·0
0·375	4·97269	0·0
0·40	5·73673	0·0
0·486175	10·0	0·0
0·559105	20·0	0·0
0·593190	40·0	0·0
0·597752	50·0	0·0
0·600793	70·0	0·0
0·60200	100·0	0·0

TABLE 4. Eigenvalues of $\tilde{\alpha}$ and R for $\sigma = 0{\cdot}50$ and $\tilde{c}_r = 0$.

required extremely accurate asymptotic solutions, which are difficult to obtain because the asymptotic series for the velocity profile converges slowly. Otherwise, if the starting solutions are not sufficiently accurate, a numerical error will grow exponentially due to the very large higher derivatives of the unbounded solutions. However, if the integration is started at a large distance, where higher order terms are negligibly small, backward integration is quite satisfactory. Both methods have been used and almost identical eigenvalues have been obtained. Backward integration uses about $\frac{2}{3}$ the computing time, as compared with forward integration, and both methods were found quite satisfactory for R up to 80. For larger R, calculations may not be very accurate due to the rapidly varying nature of the solutions. Taylor series stepwise integration was used, and the first ten terms of the series were taken to extrapolate the value of g;

$\tilde{\alpha}$	R	$\tilde{\alpha}\tilde{c}_i$	$\tilde{\alpha}$	R	$\tilde{\alpha}\tilde{c}_i$
0·8	0·696308	0·0	0·106096	11·0	0·050
0·20	2·16668	0·0	0·15	6·76547	0·050
0·30	4·06091	0·0	0·351965	11·0	0·050
0·40	7·38146	0·0	0·446625	20·0	0·050
0·472826	12·0	0·0	0·510478	40·0	0·050
0·509090	16·0	0·0	0·536226	80·0	0·050
0·531426	20·0	0·0			
0·577363	40·0	0·0	0·128	40·0	0·075
0·589956	80·0	0·0	0·18	14·6689	0·075
			0·25	12·6003	0·075
0·0346887	70·0	0·025	0·35	16·9433	0·075
0·037046	40·0	0·025	0·437655	30·0	0·075
0·0391451	20·0	0·025	0·50	79·5108	0·075
0·0423097	12·0	0·025			
0·05	5·46667	0·025	0·175	52·2647	0·10
0·065	2·97352	0·025	0·25	25·7593	0·10
0·10	2·41039	0·025	0·37	36·3	0·10
0·20	3·4	0·025	0·42	53·9579	0·10
0·315	6·0	0·025			
0·427273	12·0	0·025	0·24	85·5473	0·125
0·546789	40·0	0·025	0·32	62·4827	0·125
			0·10	1·27793	0·01
0·0680593	80·0	0·050	0·20	2·59675	0·01
0·0799916	30·0	0·050	0·20	3·15772	0·02

TABLE 5. Eigenvalues of $\tilde{\alpha}$ and R for $\sigma = 0{\cdot}25$ and $\tilde{c}_r = 0$.

$\tilde{\alpha}$	R	$\tilde{\alpha}\tilde{c}_i$	$\tilde{\alpha}$	R	$\tilde{\alpha}\tilde{c}_i$
0·08	0·961793	0·0	0·40	18·1346	0·025
0·20	3·12286	0·0	0·504688	40·0	0·025
0·30	6·10800	0·0			
0·36	9·06414	0·0	0·0680661	40·0	0·040
0·470315	20·0	0·0	0·0891865	15·0	0·040
0·541869	40·0	0·0	0·14	8·15815	0·040
			0·212971	8·5	0·040
0·04	0·851737	0·01	0·30	11·9	0·040
			0·389930	20·0	0·04
0·0185	40·0	0·015	0·478789	40·0	0·04
0·191949	4·2	0·015			
0·050	1·95214	0·015	0·107246	40·0	0·06
0·0972284	2·5	0·015	0·139936	20·0	0·06
0·294388	7·5	0·015	0·22	14·5294	0·06
0·403850	15·0	0·015	0·326850	20·0	0·06
			0·437571	40·0	0·06
0·0433774	40·0	0·025	0·16	41·0484	0·08
0·0549767	10·0	0·025	0·25	25·5223	0·08
0·085	4·63629	0·025	0·381187	40·0	0·08
0·10	4·39413	0·025			
0·14	4·54064	0·025	0·31	47·7070	0·10
0·248580	7·0	0·025	0·225	52·3278	0·10

TABLE 6. Eigenvalues of $\tilde{\alpha}$ and R for $\sigma = 0{\cdot}10$ and $\tilde{c}_r = 0$.

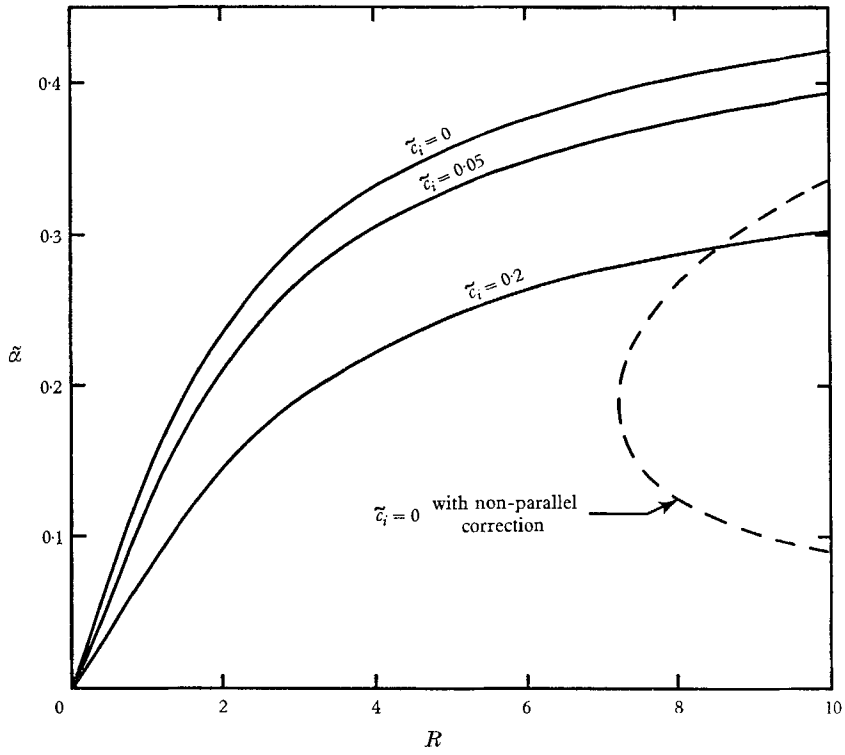

FIGURE 6. $\tilde{\alpha}$–R curves for laminar flow.

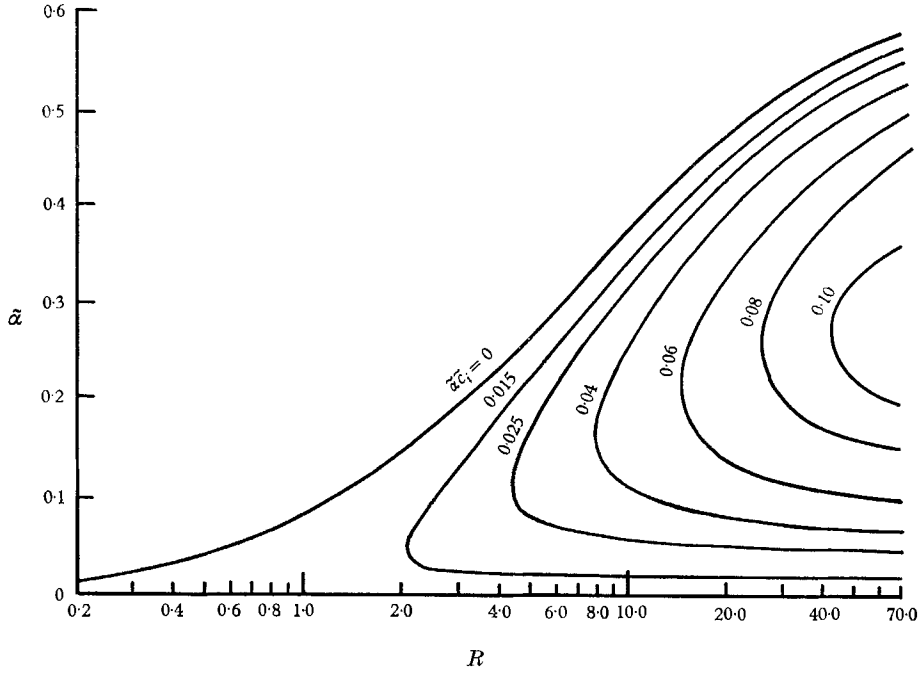

FIGURE 7. $\tilde{\alpha}$–R curves for parallel flow and $\sigma = 0{\cdot}10$.

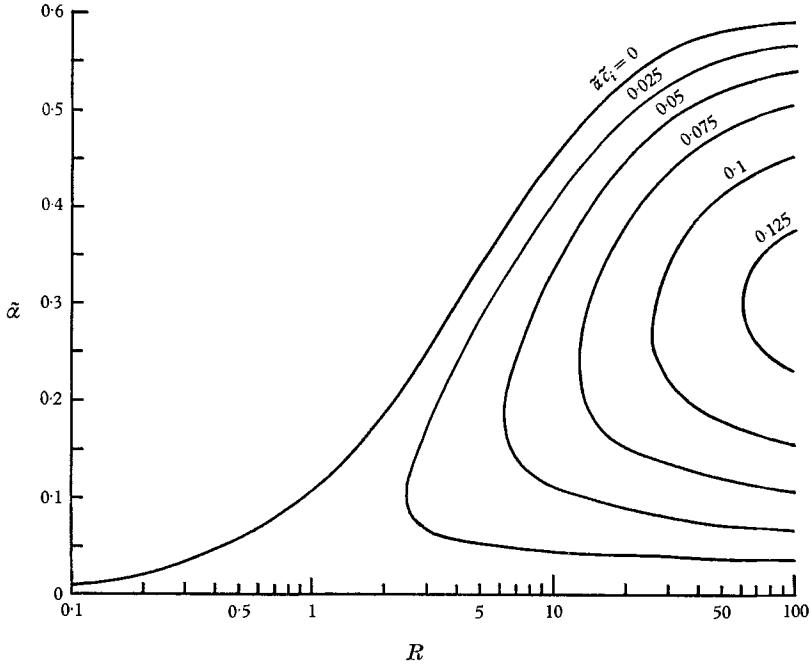

FIGURE 8. $\tilde{\alpha}$–R curves for parallel flow and $\sigma = 0{\cdot}25$.

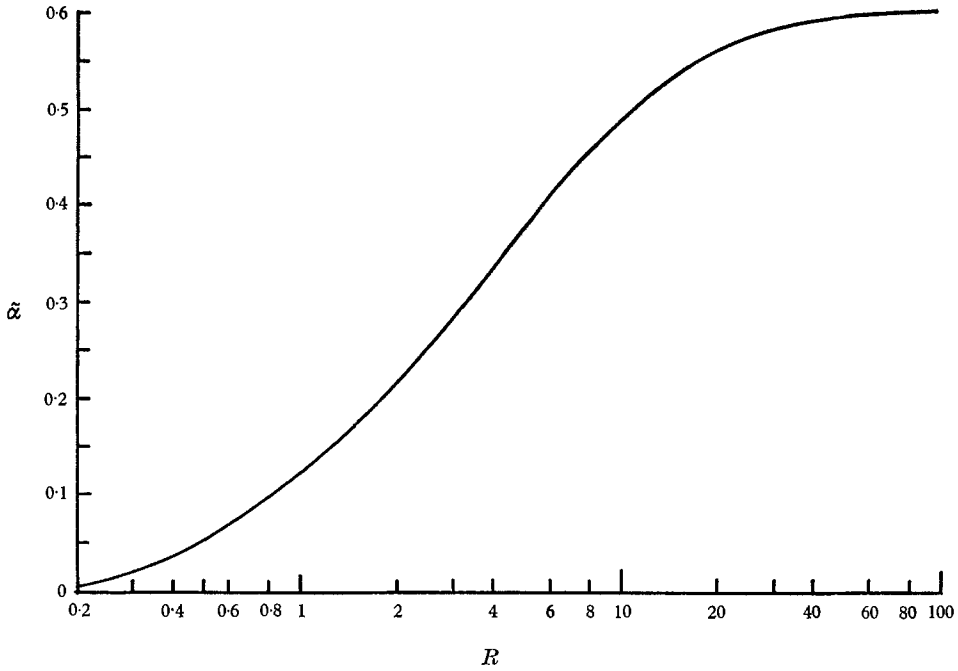

FIGURE 9. $\tilde{\alpha}$–R curve for parallel flow and $\sigma = 0{\cdot}50$.

both neutrally stable and uniformly growing disturbances were studied. Eigenvalues are tabulated in tables 4–6, and various stability curves are drawn in figures 6–9 and 11.

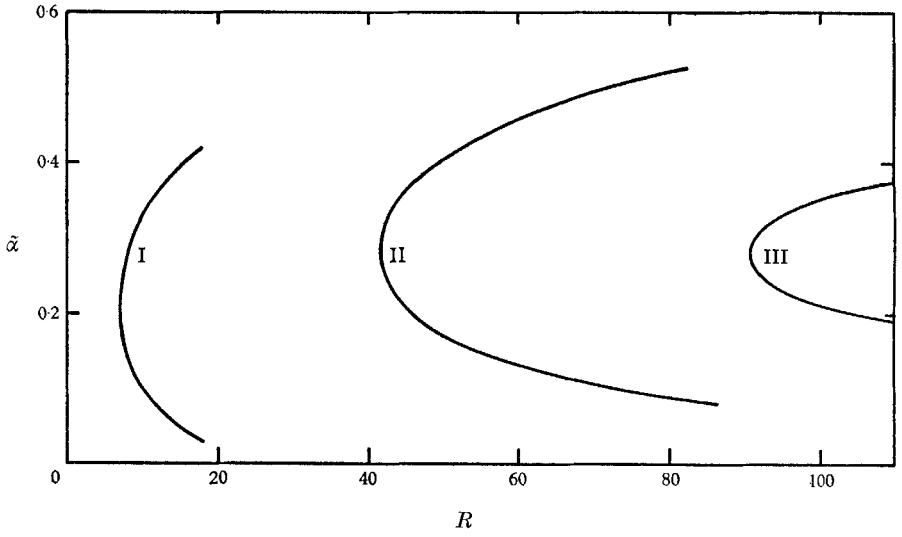

FIGURE 10. Neutral $\tilde{\alpha}$–R curves with non-parallel correction: (I) $\sigma = \infty$; (II) $\sigma = 0{\cdot}25$; (III) $\sigma = 0{\cdot}1$.

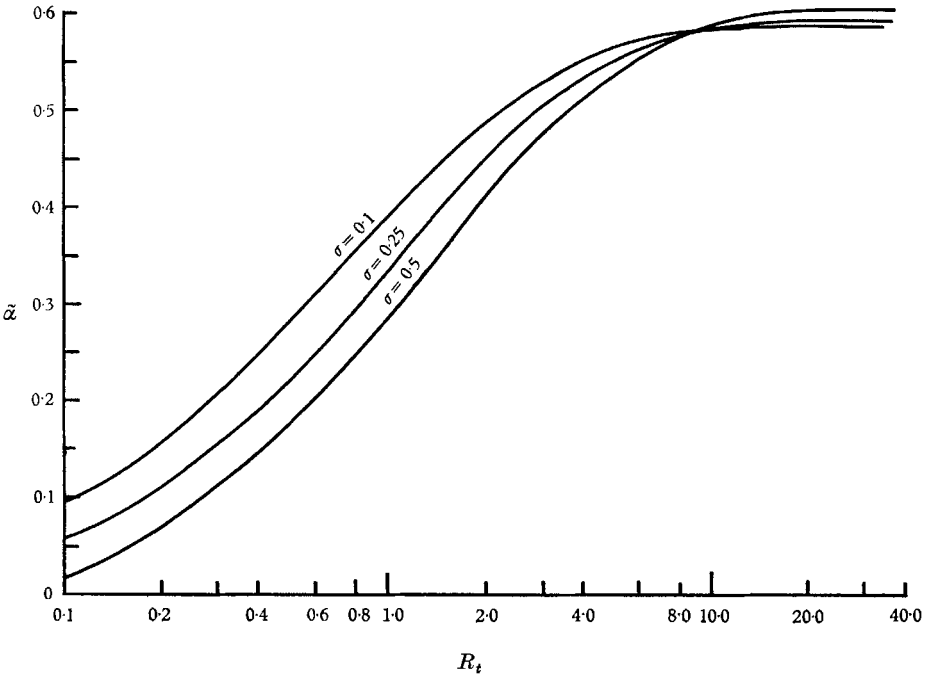

FIGURE 11. Neutral $\tilde{\alpha}$–R_t curves for parallel flow and various eddy-viscosity ratios.

6. Non-parallel flow correction

The Orr–Sommerfeld equation has been derived under the assumption that the flow is parallel. At large Reynolds number, the growth of the boundary-layer thickness is relatively small, and the flow at a given distance may be regarded as parallel. However, at low Reynolds number, there is a strong divergence of the streamlines of the main flow; the non-parallel effect has to be taken into account. For a free boundary-layer flow, the critical Reynolds number is usually expected to be small; however, it may still be of the order 5–10, and the growth of the boundary-layer thickness is not extremely large. Therefore, a first-order non-parallel correction to the values obtained from the stability of a parallel flow will be considered. In the linear stability theory, it is the interaction energy between the disturbance and the main flow that plays a role in the stability of the flow. Let the interaction energy density per unit volume be

$$E = \mathrm{Re}[E_1(y)\exp\{i(\alpha x+\beta z+\gamma y-\alpha ct)\}]. \tag{64}$$

Then the local time rate of change of the energy density is

$$\frac{\partial E}{\partial t} = \alpha c_i E.$$

The growth of the boundary-layer thickness tends to dilute the interaction energy density in the boundary layer. To the first order,

$$\left(\frac{\Delta E}{E}\right)_{\text{dilution}} = -\frac{\Delta l}{l}, \tag{65}$$

where $l = (\nu x^*/\overline{U}_1)^{\frac{1}{2}}$ is the characteristic thickness of the boundary layer and E is a dimensional quantity. Therefore

$$\left(\frac{\partial E}{\partial t}\right)_{\text{dilution}} = -\frac{E}{l}\frac{dl}{dx^*}\frac{dx^*}{dt}. \tag{66}$$

Now,
$$\frac{dx^*}{dt} = \frac{dx^*}{dt}\frac{l}{\overline{U}_1} \quad \text{and} \quad \frac{1}{l}\frac{dl}{dx^*} = \frac{1}{2x^*}.$$

Thus
$$\left(\frac{\partial E}{\partial t}\right)_{\text{dilution}} = -E/2R.$$

The time rate of change of the energy density, taking into account the boundary layer growth, is then

$$\left(\frac{\partial E}{\partial t}\right)_{\text{non-parallel}} = \left(\frac{\partial E}{\partial t}\right)_{\text{parallel}} - \frac{E}{2R}. \tag{67}$$

Thus, with this correction,

$$(\alpha c_i)_{\text{non-parallel}} = (\alpha c_i)_{\text{parallel}} - \frac{1}{2R}. \tag{68}$$

The same correction can be made for the turbulent flow. In a fully developed turbulent flow the characteristic length is inversely proportional to x^*; therefore, the correction for a turbulent shear layer is

$$(\alpha c_i)_{\text{non-parallel}} = (\alpha c_i)_{\text{parallel}} - \frac{1}{R_t}, \tag{69}$$

where R_t is the Reynolds number based on the total viscosity at the centre of the mixing layer.

The corrected neutral stability curves for $\sigma = 0{\cdot}10$, $\sigma = 0{\cdot}25$ and $\sigma = \infty$ have been plotted in figure 10. With this correction, it has been found that the neutral curves, which pass through the origin for parallel flow, do not pass through the origin with the non-parallel correction. The minimum critical Reynolds numbers are tabulated in table 3. For laminar flow, the neutral stability curve and curves corresponding to unstable disturbances ($\tilde{c}_i = 0{\cdot}05$, $0{\cdot}2$) are given in figure 6. The neutral stability curve agrees very well with that obtained by Yamada (1965), when converted to his length scale. The neutral stability curve with the non-parallel correction is shown in figure 6.

7. Discussion

Numerical calculations have been performed for the case where $|\overline{U}_1^*| = |\overline{U}_2^*|$ and $\theta = \theta_1 = \theta_2 = 45°$. The results can be easily extended to the cases with arbitrary angle θ, by proper scaling of the reference velocity and the reference length. IBM 1130 and IBM 360 computers were used for the stability calculations. Ten digit accuracy was maintained for computing mean turbulent velocity profiles.

For $R < 80$, $\tilde{\alpha}$ is a monotonically increasing function of R, and the neutral $\tilde{\alpha}$–R curve passes through the origin in all cases. The behaviour of the $\tilde{\alpha}$–R curve, for small $\tilde{\alpha}R$, is similar to that found by Esch (1957). This is because our velocity profiles, with the small second derivative of the velocity at the centre of the flow, and a rapid approach of mean velocity to free stream velocity at its edge, have a characteristic similar to Esch's velocity profile. The non-parallel correction has a stabilizing effect, and the neutral stability curve, with this correction, does not pass through the origin.

We also note that the maximum value of the non-dimensional wave-number is approximately equal to 0·6. Thus the length scale of the disturbance $\simeq 10{\cdot}45$, the characteristic length of the flow. This supports our assumption that the length scale of the oscillations is large compared with the length scale of the turbulent eddies, and it is therefore reasonable to assume the same form for eddy viscosity as that used to express the interaction of the mean flow with turbulence.

From various $\tilde{\alpha}$–R curves, we conclude that laminar and turbulent shear layers under our investigation are unstable for small wavy disturbances with a parallel flow configuration, as well as with a non-parallel flow correction. From neutral $\tilde{\alpha}$–R_t curves (figure 11), we conclude that, for small R_t, increasing eddy viscosity has a destabilizing effect, whereas at large R_t eddy viscosity has a stabilizing effect. At small R_t, once the flow is unstable, suitable components of the existing turbulence grow and develop into a large eddy system, which causes rapid entrainment (Townsend 1966). The rapid entrainment leads to an increase of turbulence intensity, and thus a decrease in σ (figure 11), making the flow stable to the growth of large eddies, and causing existing eddies to lose energy. During this period, the entrainment is weak, so that the intensity decreases until the flow is unstable to the development of large eddies of suitable scale. The cycle recurs;

the flow width and the size of the eddies also increases, which gives rise to a turbulent burst. The value of σ continues to decrease, and the characteristic length continues to increase. At a given R, the flow traces a path on which R_t decreases, $\tilde{\alpha}$ increases and σ decreases (figure 11). Thus, when $\sigma \to 0$, the flow may eventually leave the instability region. The deficiency of the linear stability analysis leads to the belief that the primary instability of the Tollmien–Schlichting type at small R_t gives rise to a secondary instability of the Taylor–Goertler type.

The research for this paper was supported in part by a grant from the National Science Foundation.

Appendix

Phase velocity of disturbances

For plane Poiseuille flow and plane Couette flow, Synge (1938) obtained a sufficient condition for stability. This condition was later extended to flows with infinite boundary conditions by Lessen (1952) and Pai (1954). However, Pai's results, which indicate that a minimum critical Reynolds exists for a free boundary layer, does not apply to a velocity profile of an odd function.

Multiplying (37) by the complex conjugate of g, and integrating from $y = -\infty$ to $y = \infty$, one obtains

$$i\tilde{\alpha}R\tilde{c}(I_1^2+\tilde{\alpha}^2I_0^2) = I_2^2+2\tilde{\alpha}^2I_1^2+\tilde{\alpha}^4I_0^2+1/\sigma\left[\int_{-\infty}^{\infty} G(g''\bar{g}''+2\tilde{\alpha}^2g'\bar{g}')\,dy + \tilde{\alpha}^2\int_{-\infty}^{\infty} G''g\bar{g}\,dy\right]+i\tilde{\alpha}RQ, \quad \text{(A 1)}$$

where
$$I_0^2 = \int_{-\infty}^{\infty} g\bar{g}\,dy, \quad I_1^2 = \int_{-\infty}^{\infty} g'\bar{g}'\,dy, \quad I_2^2 = \int_{-\infty}^{\infty} g''\bar{g}''\,dy,$$
$$Q = \int_{-\infty}^{\infty} [\bar{U}g'\bar{g}'+\bar{U}'\bar{g}g'+(\tilde{\alpha}^2\bar{U}+\bar{U}'')g\bar{g}']\,dy,$$

and the superscript 'bar' denotes the complex conjugate quantity.

The imaginary part of (A 1) is

$$\tilde{\alpha}R\tilde{c}_r(I_1^2+\tilde{\alpha}^2I_0^2) = \tilde{\alpha}R[\mathrm{Re}\,(Q)]. \quad \text{(A 2)}$$

If $\bar{U}$ is an odd function and $\bar{U}'$ vanishes at the boundaries

$$Q = \int_{-\infty}^{\infty} \bar{U}'\bar{g}'g\,dy = -\int_{-\infty}^{\infty} \bar{U}'g'\bar{g}\,dy.$$

Hence, Q is pure imaginary. Since I_0^2 and I_1^2 are both real and positive, the phase velocity of disturbances must vanish for the flow with an odd velocity profile.

Lower bound of the neutral stability curves

The real part of (A 1) is

$$-\tilde{\alpha}R\tilde{c}_i(I_1^2+\tilde{\alpha}^2I_0^2) = I_2^2+2\tilde{\alpha}^2I_1^2+\tilde{\alpha}^4I_0^2+1/\sigma\left[\int_{-\infty}^{\infty} G(g''\bar{g}''+2\tilde{\alpha}^2g'\bar{g}'+\tilde{\alpha}^4g\bar{g})\,dy + \tilde{\alpha}^2\int_{-\infty}^{\infty} G''g\bar{g}\,dy\right]-\tilde{\alpha}R[\mathrm{Im}\,(Q)]. \quad \text{(A 3)}$$

It can be shown that

$$|\mathrm{Im}\,(Q)| < q^* I_0 I_1, \tag{A 4}$$

where

$$q^* = |\bar{U}'|_{\max}.$$

Now, for real positive constants a and b,

$$\int_{-\infty}^{\infty} (g + a\bar{U}'g' + bg'')(\bar{g} + a\bar{U}'\bar{g}' + b\bar{g}'')\,dy > 0.$$

For an odd function $\bar{U}$, the above inequality reduces to

$$b^2 I_2^2 > I_1^2(2b - a^2 q^{*2}) - I_0^2. \tag{A 5}$$

Since $G(\eta)$ is a positive, even function for the flow under consideration, and since $|G(\eta)|_{\max} = 1$, one can set

$$\int_{-\infty}^{\infty} G(g''\bar{g}'' + 2\tilde{\alpha}^2 g'\bar{g}' + \tilde{\alpha}^4 g\bar{g})\,dy = G^*(I_2^2 + 2\tilde{\alpha}^2 I_1^2 + \tilde{\alpha}^4 I_0^2) \quad (0 < G^* < 1). \tag{A 6}$$

For the assumed function $G(\eta)$ (§5.1), (G'') minimum $= -2A$; therefore one can write

$$\int_{-\infty}^{\infty} G''g\bar{g}\,dy > -2AI_0^2, \tag{A 7}$$

where A is real and positive.

By substituting (A 4)–(A 5) into (A 3), one obtains

$$\tilde{\alpha}R\tilde{c}_i(I_1^2 + \tilde{\alpha}^2 I_0^2) < -\left(1 + \frac{G^*}{\sigma}\right)\left[\left(2\tilde{\alpha}^2 + \frac{2}{b} - \frac{a^2}{b^2}q^{*2}\right)I_1^2 + \left(\tilde{\alpha}^4 - \frac{1}{b^2} - \frac{2A\tilde{\alpha}^2}{\sigma + G^*}\right)I_0^2\right] + \tilde{\alpha}Rq^* I_0 I_1. \tag{A 8}$$

For stability $\tilde{c}_i < 0$, the right-hand side of the above inequality should be negative; therefore one has

$$(\tilde{\alpha}Rb^2q^*)^2 < 4\left(1 + \frac{G^*}{\sigma}\right)^2 (2\tilde{\alpha}^2 b^2 + 2b - a^2 q^{*2})\left(\tilde{\alpha}^4 b^2 - 1 - \frac{2A\tilde{\alpha}^2}{\sigma + G^*}b^2\right), \tag{A 9}$$

where a and b satisfy

$$\left.\begin{aligned} &2\tilde{\alpha}^2 b^2 + 2b - a^2 q^{*2} > 0, \\ \text{and} \quad &\tilde{\alpha}^4 b^2 - 1 - \frac{2A\tilde{\alpha}^2}{\sigma + G^*}b^2 > 0. \end{aligned}\right\} \tag{A 10}$$

For $\tilde{\alpha}^2 > 2A/(\sigma + G^*)$ one chooses

$$a = 0, \quad b = K/\tilde{\alpha}^2, \tag{A 11}$$

where

$$K^2 > \frac{1}{1 - (2A/x^2(\sigma + G^*))}.$$

The conditions (A 10) are satisfied, and (A 9) becomes

$$(Rq^*)^2 < \frac{8\tilde{\alpha}^4}{K^3}\left(1 + \frac{G^*}{\sigma}\right)^2 (K + 1)\left(K^2 - 1 + \frac{2A}{\sigma + G^*}\frac{K^2}{\tilde{\alpha}^2}\right). \tag{A 12}$$

This condition gives a lower bound for stability. As it is seen that when $\tilde{\alpha}$ becomes small, R is also small. The neutral stability curve may pass through the

origin of the $\tilde{\alpha}$–R diagram. From all calculations for the laminar flow performed to date, it actually does. However, when $\tilde{\alpha}^2 < 2A/(\sigma+G^*)$ (A 10) does not hold. The lower bound for stability is not obtained.

REFERENCES

Esch, R. E. 1957 *J. Fluid Mech.* **3**, 289.

Lessen, M. 1950 *NACA Rep.* no. 979

Lessen, M. 1952 *Quart. Appl. Math.* **10**, 184.

Liepman, W. H. & Laufer, J. 1947 *NACA TN* no. 1237.

Malkus, W. 1956 *J. Fluid Mech.* **1**, 521.

Pai, S. I. 1954 *Quart. Appl. Math.* **12**, 203.

Reynolds, W. C. & Tiederman, W. G. 1967 *J. Fluid Mech.* **27**, 253.

Squire, H. B. 1933 *Proc. Roy. Soc.* A **142**, no. A 847, Ser. A, 621.

Synge, J. L. 1938 *Semi-centennial Publications of the American Mathematical Society*, **2**, 227.

Townsend, A. A. 1956 *The Structure of Turbulent Shear Flow*. Cambridge University Press.

Townsend, A. A. 1966 *J. Fluid Mech.* **26**, 689.

Yamada, H. 1960 *Rep. Res. Inst. Appl. Mech.* **8**, 30, 1.

Yamada, H. 1965 *Rep. Res. Inst. Appl. Mech.* **13**, 45, 1.